OTFS Modulation and Influence of Wideband RF Impairments Measured on a 60 GHz Testbed

Roman Marsalek*, Jiri Blumenstein*†, Daniel Schützenhöfer†, Martin Pospisil*
*Department of Radio Electronics, Brno University of Technology, Czech Republic
†Christian Doppler Laboratory for Dependable Wireless Connectivity for the Society in Motion, Institute of Telecommunications, TU Wien
{marsaler, blumenstein, xpospi29}@feec.vutbr.cz, daniel.schuetzenhoefer@nt.tuwien.ac.at

***Abstract*—Orthogonal Time Frequency Space (OTFS) modulation has recently been proposed for communication in doubly selective channels. Together with millimeter waves, OTFS seems to be one of the promising candidates for beyond-5G communication systems. In this paper we present the performance of an OTFS system with an Linear Minimum Mean Square Error (LMMSE) equalizer in the presence of main hardware impairments extracted from our millimeter-wave setup in the 60 GHz band.**

***Index Terms*—OTFS, hardware impairments, millimeter-waves, nonlinearity, 60 GHz testbed**

I. Introduction

The recently proposed technique - Orthogonal Time Frequency Space (OTFS) [1] modulation is a two-dimensional modulation format claiming excellent performance in doubly-selective wireless channels, in which Orthogonal Frequency Division Multiplexing (OFDM) suffers from an important error floor.

In OTFS, the two-dimensional precoding and postprocessing blocks are added on top of the conventional OFDM modulator/demodulator [2] and the data symbols (usual inner mapping is M-QAM) are placed in a delay-Doppler domain. This well corresponds to the nature of wireless channels with scattering objects manifesting in multipath components affected by Doppler shifts due to either the transmitter or receiver moving, or the environment.

Due to spectrum scarcity in traditional bands below 6 GHz, the millimeter wave frequencies become attractive for 5G and beyond systems. But the performance of any communication link is affected by the presence of hardware imperfections such as power amplifier nonlinearity, quadrature (IQ) modulator/demodulator imbalances or phase noise. In [3] we have shown how the millimeter-wave channel capacity is affected by the realistic, i.e., measured IQ imbalances of 60 GHz modulators. In [4], we have presented our digitally calibrated 60 GHz setup for research of power amplifier linearization techniques, which we subsequently used for digital predistorion evaluations [5]. Performance evaluations of OTFS at 5G millimeter-wave frequencies has been published in [6], where it has been shown that OTFS exhibits a lower Bit Error Rate (BER) than OFDM in the numerous situations. The influence of phase noise on OTFS has been analyzed in [7].

In contrast to OFDM, where the pilot tones for channel estimation are interleaved with the data in the time-frequency plane, the embedded pilot in the delay-Doppler domain has been proposed recently for use in OTFS [8]. Due to the nature of OTFS, such a pilot is then spread over the whole time-frequency plane. In [9], we have pointed out that an optimal data-to-pilot power allocation can be found and that such power allocation well correlates with almost the optimal Peak to Average Power Ratio (PAPR) of the transmitted signal. The distribution of PAPR of OTFS has also thoroughly been studied in [10].

The investigations presented in this paper aimed to unveil these two interesting research questions:

- How the OTFS system is sensitive to major RF front-end impairments, namely power amplifier nonlinearity and IQ imbalances?
- Which one of the effects - the RF front-end impairments or a delay-Doppler grid mismatch - determines the BER performance of OTFS?

II. Orthogonal Time Frequency Space modulation

A. OTFS modulator

The OTFS information symbols (usually M-ary QAM symbols) $x[k,l]$ placed in the delay-Doppler domain with a delay domain index $k = 0, 1..., N-1$ and a Doppler domain index $l = 0, 1, ..., M-1$ are first spread to the time-frequency domain with symbols $X[n,m]$ through a two-dimensional (2D) Inverse Symplectic Finite Fourier Transform (ISFFT) according to:

$$X[n,m] = \text{ISFFT}\left\{x[k,l]\right\} = \sum_{k=0}^{N-1}\sum_{l=0}^{M-1} x[k,l]e^{-j2\pi\left(\frac{ml}{M}-\frac{kn}{N}\right)}. \quad (1)$$

Note that the delay-Doppler symbols $x[k,l]$ can be either the data symbols $x_d[k,l]$ or the pilot symbols $x_p[k,l]$. Subsequently, the signal $X[n,m]$ is transformed from the time-frequency to the time domain by means of a Heisenberg transform:

$$x(t) = \sum_{n=0}^{N-1}\sum_{m=0}^{M-1} X[n,m]w_{TX}(t-nT)e^{j2\pi m\Delta f(t-nT)}, \quad (2)$$

where w_{TX} is a transmitter pulse shape, T and Δf are the symbol duration and tone separation that (inversely) define a quantization step in the delay and Doppler grid. Operation of

an OTFS receiver is inverse to that of the transmitter and its description can be found, e.g., in [11].

B. OTFS detector

There are several approaches for OTFS symbol detection, mainly based on the message passing approach [11] or interference cancellation [12]. Such approaches benefit from the assumption of channel sparsity in the delay-Doppler domain and aim at overcoming high computational complexity of the approach based on deconvolution [13] of the received symbols and the channel. Another approach is the LMMSE equalizer [14], that we have used during experiments described below. In our model, the received signal without equalization can be expressed in vector form such as:

$$\mathbf{r} = \mathbf{H}\mathbf{x} + \mathbf{w}, \tag{3}$$

with $\mathbf{x}, \mathbf{r}, \mathbf{w}$ being the transmitted signal, the received signal and the noise vectors of length MN, respectively and $\mathbf{H}$ is a $MN \times MN$ channel matrix. The equalized delay-Doppler domain symbols $\hat{\mathbf{d}}$ can then be expressed as [14]:

$$\hat{\mathbf{d}} = (\mathbf{H}\mathbf{A})^H \left[(\mathbf{H}\mathbf{A}) (\mathbf{H}\mathbf{A})^H + \frac{\sigma_n^2}{\sigma_d^2}\mathbf{I} \right]^{-1} \mathbf{r}, \tag{4}$$

where the channel matrix $\mathbf{H}$ can be decomposed into two main components: a diagonal Doppler matrix Δ^{k_p} and a circulant delay matrix Π^{l_p} :

$$\mathbf{H} = \sum_{p=1}^{P} h_p \Pi^{l_p} \Delta^{k_p}. \tag{5}$$

Note that P is the number of channel taps, h_p are the tap magnitudes, $\mathbf{A}$ is a modulation matrix [14], $\mathbf{I}$ is an identity matrix and $\frac{\sigma_n^2}{\sigma_d^2}$ is the noise-to-signal ratio estimate.

For any of the data detection approaches, a reliable channel estimation method is needed. The most convenient way is to use a pilot-based approach, where the pilot frames are interleaved with data frames. In such a case, the channel state information may become obsolete in highly time-varying channels, so the use of embedded pilots has been proposed in [8]. The principle of the embedded pilot is illustrated on Fig. 1. The pilot is placed at some chosen position k_p, l_p in the delay-Doppler domain and is surrounded by the guard intervals (zeros) in both domains. Remaining positions in the delay-Doppler grid serve for data transmission in form of e.g. QAM symbols.

The granularity of the delay-Doppler grid with respect to real parameters of a wireless communication channel determines the OTFS performance in various scenarios and environments. The granularity in the delay domain is $\frac{1}{M\Delta f}$, while the granularity in the Doppler domain is $\frac{1}{NT_{sym}}$, where the symbol time T_{sym} is equal to the reciprocal value of subcarrier spacing Δf. OTFS then generally performs well in the case of a real Doppler shift being the multiples of Doppler-domain granularity, while in the non-integer case, special countermeasures must be taken [8]. In the following, we will thus consider the Doppler grid mismatch as the remainder after dividing the actual Doppler shift in the channel and Doppler-domain granularity $\frac{1}{NT_{sym}}$.

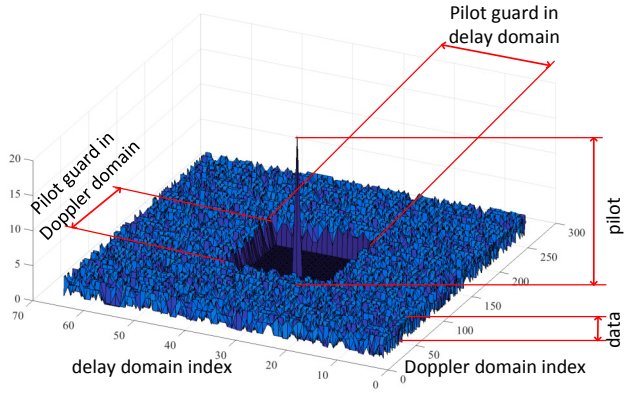

Fig. 1: Symbols in delay-Doppler domain [9]

III. Experiment

A. 60 GHz testbed description

The goal of this paper is to investigate OTFS performance in the presence of RF front-end impairments modeled, based on the parameters extracted from our millimeter-wave testbed in the 60 GHz band that we presented in [4]. Its block structure is plotted in Fig. 2.

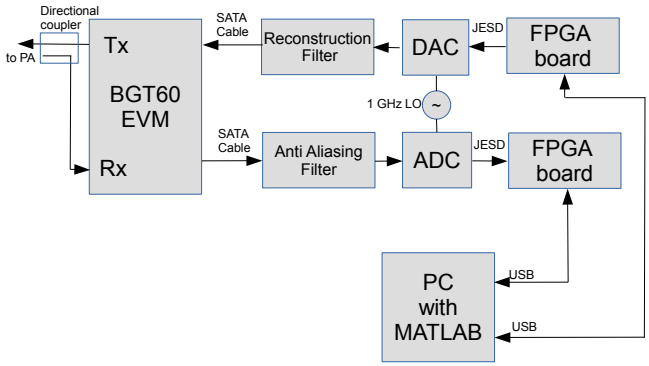

Fig. 2: Block schematic of the 60 GHz setup used for RF front-end parameters extraction [4]

The testbed is based on the Infineon BGT-60 evaluation board, a direct conversion up/down converter with up to 1 GHz bandwidth. For A/D conversion, a dual-channel ADS54j40 device (14 bit, 1.0 GSps) is used and a quad-channel DAC37j84 (16-bit, 1.6/2.5 GSPS) serves for D/A conversion. To ensure a coherent clock at Tx and Rx sides, both A/D and D/A converters are driven with a 1 GHz ultra-low-phase-noise SAW oscillator signal through a dedicated clock distributor.

B. Main RF impairments

1) Power amplifier model: Nonlinearity of the radio frequency power amplifier is one of the main sources of signal distortion in the wireless radio frequency front-ends. In order

to limit signal distortions, the power amplifiers (PA) are often used with a backoff of several decibels from saturation, that leads to a power efficiency reduction. A working point of the PA needs to be set up with respect to PAPR of the transmitted signal.

The AM/AM and AM/PM characteristics of the measured power amplifier from the BGT-60-based 60 GHz setup are shown in Fig. 3. Based on the acquired data, a memory polynomial model is identified in the form of:

$$z(t) \quad = \quad \sum_{u=1}^{U} \sum_{v=0}^{V} b_{uv} \; x(t-v)|x(t-v)|^{u-1} \qquad (6)$$

where x is the PA input signal, z is the PA output signal, b_{uv} are the polynomial coefficients with nonlinearity order U and memory depth V.

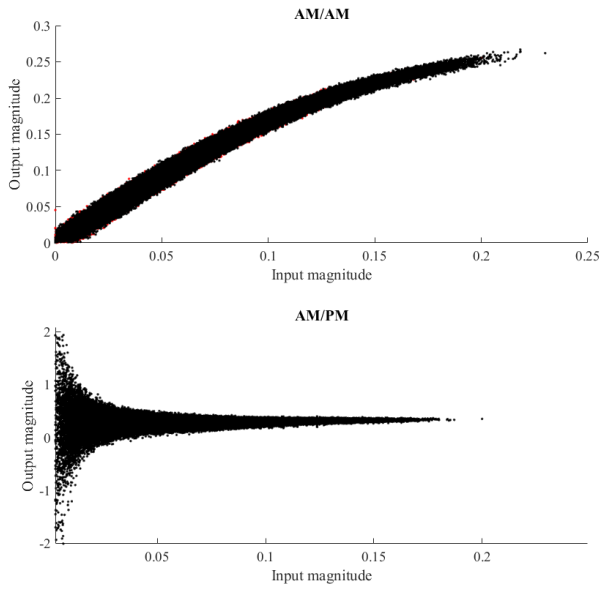

Fig. 3: Extracted AM/AM and AM/PM characteristics of 60 GHz power amplifier

2) IQ modulator imbalances: For the sake of simplicity, we have considered here the frequency-independent IQ imbalance model with an effect on the modulated signal $x(t)$ described as [15]:

$$y(t) = \alpha \cdot x(t) + \beta \cdot x^*(t), \qquad (7)$$

where $*$ denotes a complex conjugation operator, $\alpha = \cos\Delta\phi + j\epsilon\sin\Delta\phi$, $\beta = \epsilon\cos\Delta\phi - j\sin\Delta\phi$, where $\Delta\phi$ and ϵ are the phase and gain imbalance of the IQ modulator or demodulator.

The gain imbalance used in the model was set to 0.44 dB and the phase imbalance to 4 degrees, similarly to the case of our previous OFDM capacity analysis paper [3].

C. OTFS methods and parameters

The freely-available OTFS example framework [16] with a rectangular pulse shape w_{TX} was, similarly to our previous paper [9], used as a baseline for the OTFS MATLAB implementation, with the embedded pilot [8] concept for channel estimation and the LMMSE [14] channel equalizer with standard complexity, i.e., not based on matrix decomposition.

The pilot surrounded by necessary guard bands was first embedded into the delay-Doppler grid with the QAM data symbols and modulated by the OTFS modulator. The time-domain signal was then fed to the IQ modulator and power amplifier models. The effect of a linear static channel was modeled by a simplified multipath channel model with adjustable delay and Doppler parameters. Based on the channel estimation and equalization, the received QAM symbols are obtained in the OTFS demodulation block.

The results of the analysis are shown for OTFS with M=32, N=32 grid elements in the delay and Doppler domains, one embedded pilot with the power of $|x_p[k,l]|^2$ in the delay-Doppler domain, data-carrying 4-QAM symbols $x_d[k,l]$ with a mean power of $E\left\{|x_d[k,l]|^2\right\}$. The pilot power relative to the data power $\frac{P_{pilot}}{P_{data}} = \frac{|x_p[k,l]|^2}{E\left\{|x_d[k,l]|^2\right\}}$ has been set to optimal values according to our prior analysis [9]. There were N_{guard}=8 and M_{guard}=8 guards, i.e., zero symbols around the pilot selected to ensure the channel estimation is unaffected by the transmitted data.

For the sake of simplicity, the channel was modeled as a convolution of the transmitted OTFS time-domain signal with a channel impulse response having three complex-valued taps with delays of 0, 3 and 6 samples.

IV. Results

The influence of RF front-end parameters and wireless channel on the OTFS system has been evaluated in terms of BER curves. For the setup of simulation parameters of RF front-end models, OTFS and channel model description, please see Section III. We have considered three main cases, with the results shown in Fig. 4-6.

Fig. 4 shows the BER performance in the case of the wireless channel turned off, i.e., only the effects of RF front-end impairments, from which either only the power amplifier is compensated, both the power amplifier and IQ imbalance are compensated, or none of these impairments is compensated for.

The results in Fig. 5 show us, that if the Doppler shift in the wireless channel is the integer multiple of the Doppler-domain granularity, then OTFS performance is close to the performance of no channel even in the case of RF front-end impairments.

For the rectangular OTFS pulses that have been used in the simulation, the effect of non-integer Doppler shift, i.e., mismatch between the OTFS grid and real wireless channel parameters, may dominate over the effects of RF front-end imperfections, as demonstrated in the results in Fig. 6.

V. Conclusion

In this contribution, we have presented the influence of main RF front-end impairments on the Orthogonal Time Frequency

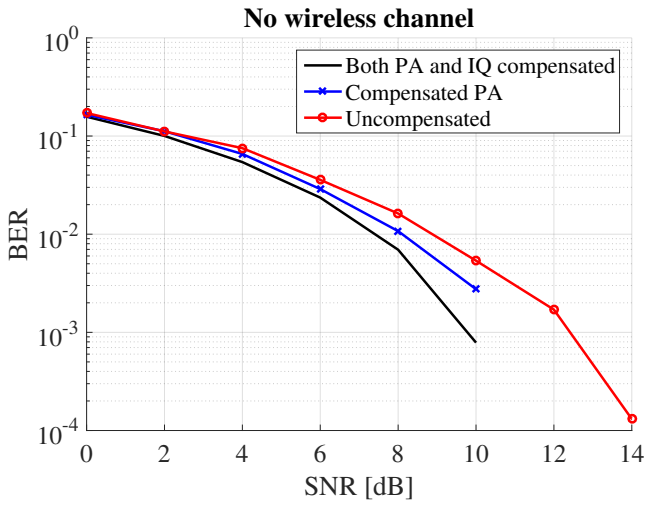

Fig. 4: Bit error rate, without channel, only RF impairments

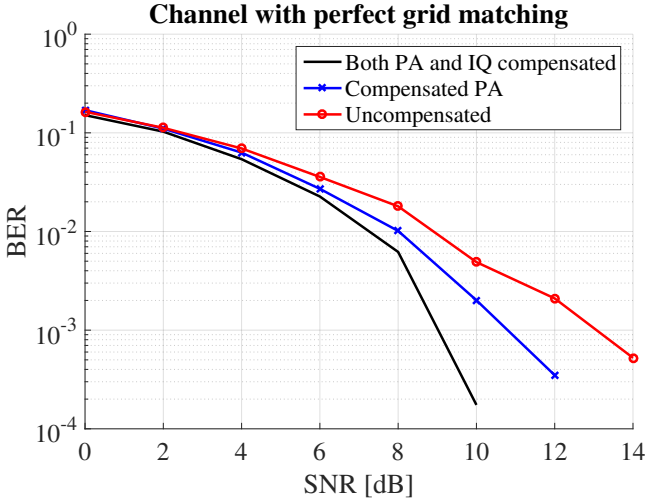

Fig. 5: Bit error rate, RF impairments and channel with perfect grid match

Space communication system. The parameters of RF front-end have been extracted from the millimeter-wave testbed working in the 60 GHz band. An LMMSE equalizer for OTFS detection has been used. We have pointed out that although the influence of RF front-end parameters may cause significant degradation of the OTFS system, there exist also some other effects, such as the non-integer Doppler shift with respect to the delay-Doppler grid, that without particular countermeasures may even have more severe influence on the overall bit error rate of the system.

Acknowledgment

This research was supported by Brno University of Technology internal project FEKT-S-20-6325 *Mobile communication systems of 5th generation and beyond*. This work was supported by the Austrian Federal Ministry for Digital and Economic Affairs and the Austrian National Foundation for Research, Technology and Development. This work was supported by the Ministry of Education, Youth and Sports (MEYS) of the Czech Republic project no. LTC18021 (FEWERCON).

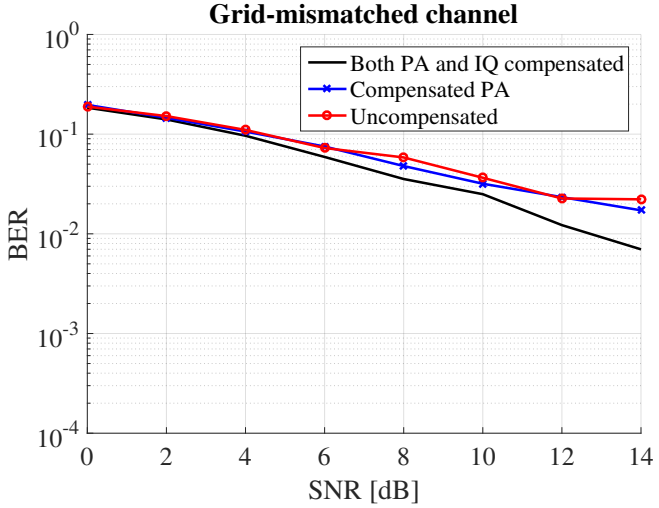

Fig. 6: Bit error rate, RF impairments and channel with grid mismatch of 20%

References

[1] R. Hadani, S. Rakib, M. Tsatsanis, A. Monk, A. J. Goldsmith, A. F. Molisch, and R. Calderbank, "Orthogonal time frequency space modulation," in *2017 IEEE Wireless Communications and Networking Conference (WCNC)*, IEEE, 2017, pp. 1–6.

[2] A. RezazadehReyhani, A. Farhang, M. Ji, R. R. Chen, and B. Farhang-Boroujeny, "Analysis of discrete-time MIMO OFDM-based orthogonal time frequency space modulation," in *2018 IEEE International Conference on Communications (ICC)*, IEEE, 2018, pp. 1–6.

[3] R. Marsalek, J. Blumenstein, M. Pospisil, and M. Rupp, "Measured capacity of mm-wave radio link under IQ imbalance," in *2018 IEEE 29th Annual International Symposium on Personal, Indoor and Mobile Radio Communications (PIMRC)*, IEEE, 2018, pp. 1124–1125.

[4] R. Maršálek, M. Pospıšil, T. Gotthans, and T. Urbanec, "Digital calibration of 60 GHz setup for use in power amplifier predistortion," in *2019 IEEE 20th International Workshop on Signal Processing Advances in Wireless Communications (SPAWC)*, IEEE, 2019, pp. 1–4.

[5] J. Kral, T. Gotthans, R. Marsalek, M. Harvanek, and M. Rupp, "On feedback sample selection methods allowing lightweight digital predistorter adaptation," *IEEE Transactions on Circuits and Systems I: Regular Papers, in print*, 2020.

[6] R. Hadani, S. Rakib, A. Molisch, C. Ibars, A. Monk, M. Tsatsanis, J. Delfeld, A. Goldsmith, and R. Calderbank, "Orthogonal time frequency space (OTFS) modulation for millimeter-wave communications systems," in *2017 IEEE MTT-S International Microwave Symposium (IMS)*, IEEE, 2017, pp. 681–683.

[7] G. Surabhi, M. K. Ramachandran, and A. Chockalingam, "OTFS modulation with phase noise in mmWave communications," in *2019 IEEE 89th Vehicular Technology Conference (VTC2019-Spring)*, IEEE, 2019, pp. 1–5.

[8] P. Raviteja, K. T. Phan, and Y. Hong, "Embedded pilot-aided channel estimation for OTFS in Delay–Doppler channels," *IEEE Transactions on Vehicular Technology*, vol. 68, no. 5, pp. 4906–4917, 2019.

[9] R. Marsalek, J. Blumenstein, A. Prokes, and T. Gotthans, "Orthogonal time frequency space modulation: Pilot power allocation and nonlinear power amplifiers," in *2019 IEEE International Symposium on Signal Processing and Information Technology (ISSPIT)*, IEEE, 2019, pp. 1–4.

[10] G. Surabhi, R. M. Augustine, and A. Chockalingam, "Peak-to-average power ratio of OTFS modulation," *IEEE Communications Letters*, vol. 23, no. 6, pp. 999–1002, 2019.

[11] P. Raviteja, K. T. Phan, Q. Jin, Y. Hong, and E. Viterbo, "Low-complexity iterative detection for orthogonal time frequency space modulation," in *2018 IEEE Wireless Communications and Networking Conference (WCNC)*, IEEE, 2018, pp. 1–6.

[12] T. Zemen, M. Hofer, D. Loeschenbrand, and C. Pacher, "Iterative detection for orthogonal precoding in doubly selective channels," in *2018 IEEE 29th Annual International Symposium on Personal, Indoor and Mobile Radio Communications (PIMRC)*, IEEE, 2018, pp. 1–7.

[13] S. S. Rakib and R. Hadani, *Orthogonal time frequency space communication system compatible with OFDM*, US Patent 10,411,843, Sep. 2019.

[14] S. Tiwari, S. S. Das, and V. Rangamgari, "Low complexity LMMSE receiver for OTFS," *IEEE Communications Letters*, vol. 23, no. 12, pp. 2205–2209, 2019.

[15] J. Tubbax, B. Come, L. Van der Perre, L. Deneire, S. Donnay, and M. Engels, "Compensation of IQ imbalance in OFDM systems," in *IEEE International Conference on Communications, 2003. ICC '03.*, vol. 5, May 2003, 3403–3407 vol.5.

[16] P. Raviteja, K. T. Phan, Y. Hong, and E. Viterbo, "Interference cancellation and iterative detection for orthogonal time frequency space modulation," *IEEE Transactions on Wireless Communications*, vol. 17, no. 10, pp. 6501–6515, 2018.